

# Particle identification of projectilelike residues

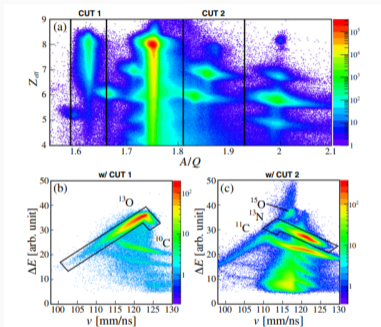


FIG. 1. Particle identification of projectilelike residues. Particle's velocity ( $v$ ) is deduced from TOF. Combining  $B\rho$  and velocity allows to determine particle's mass-to-charge ratio  $A/Q$ .  $Z_{eff}$  is the deduced effective atomic number with  $\Delta E$  and velocity using the Bethe-Bloch formula. The energy deposit of a charged particle in a material is related to its velocity, charge, and mass, as shown in the  $\Delta E$ - $v$  spectra with (w/) the  $A/Q$  selections from 1.59 to 1.66 (b) and from 1.81 to 1.93 (c). Black contours in (b) and (c) select  $^{13}\text{O}$  and  $^{13}\text{N}$ , respectively.

$^{13}\text{O}$ :  $A/Q = 1.625$ ,  $^{14}\text{O}$ :  $A/Q = 1.75$ .

TOF  $\rightarrow v$ ;  $B\rho \rightarrow \frac{A}{Q}$ ;  $\Delta E, v \rightarrow Z_{eff}$

$Z_{eff}$ : the deduced effective atomic number.

(a): Tails of  $^{14}\text{O}$  and  $^{13}\text{O}$  extending to smaller  $Z_{eff}$  region, since:

- $^{14}\text{O}$ : unreacted projectiles interacting in the hodoscope
- $^{13}\text{O}$ : low-energy  $^{13}\text{O}$  stopped in the hodoscope.

(b): most  $^{13}\text{O}$  stopped in the hodoscope,  $\Delta E$  proportional to velocity.

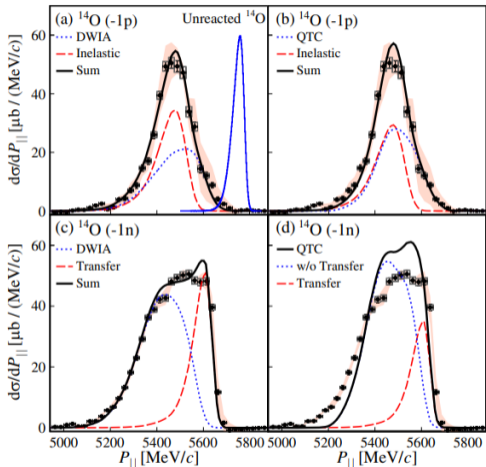
(c): most  $^{13}\text{N}$  punched through the hodoscope,  $\Delta E$  antiproportional to velocity.

# Experimental and theoretical cross sections for one-nucleon removal from $^{14}\text{O}$

TABLE I. Experimental ( $\sigma_{\text{exp}}$ ) and theoretical ( $\sigma_{\text{th}}$ ) cross sections for one-nucleon removal from  $^{14}\text{O}$  at 94 MeV/nucleon. SF represents the spectroscopic factor from shell-model calculations (see SM [58]). The reduction factors  $R_s = \sigma_{\text{exp}}/\sigma_{\text{th}}$  are also given.

Residue	$J^\pi$	$\sigma_{\text{exp}}$ (mb)	SF	Theory	$\sigma_{\text{sp}}$ (mb)	$\sigma_{\text{th}}$ (mb)	$R_s$
$^{13}\text{N}_{\text{g.s.}}$	$1/2^-$	10.7(16)	1.58	DWIA	5.2	8.8	1.22(18)
				Inelastic	...	9	
				Sum		17.8	0.60(9)
				QTC	7.0	11.9	0.90(13)
				Inelastic	...	9	
				Sum		20.9	0.51(8)
$^{13}\text{O}_{\text{g.s.}}$	$3/2^-$	16.7(24)	3.42	DWIA	6.3	23.2	0.72(10)
				Transfer	3	11	
				Sum		34.2	0.49(7)
				QTC	10.2	37.6	0.44(6)
				w/o transfer			
QTC	13.5	49.7	0.34(5)				

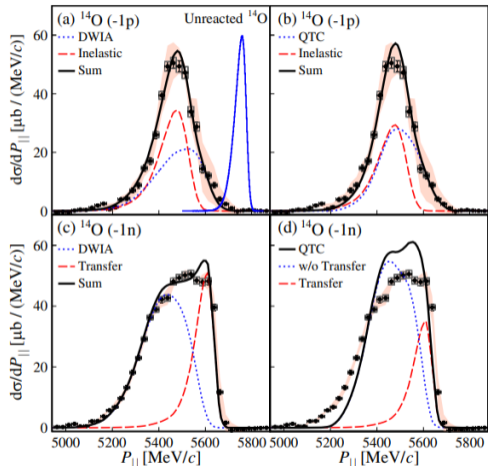
# Parallel momentum distributions of $^{13}\text{N}$ and $^{13}\text{O}$



$$^{14}\text{O}(p, 2p)^{13}\text{N} \quad \text{and} \quad ^{14}\text{O}(p, pn)^{13}\text{O}$$

- Comparison of DWIA and QTC calculation.
- Key difference is how they handle three body final state:
- DWIA: product of the  $p$ -residue and  $N$ -residue states.
- QTC: expands in terms of  $p - N$  states, include deuteron ground state for  $1n$  removal.

# Parallel momentum distributions of $^{13}\text{N}$ and $^{13}\text{O}$



Blue solid line: distribution of the unreacted  $^{14}\text{O}$ . Shift by  $-200 \text{ MeV}/c$ , broadened of the momentum.

Symmetrical properties:

(a)(b)

(loosely bound) 1p removal: close to symmetric.

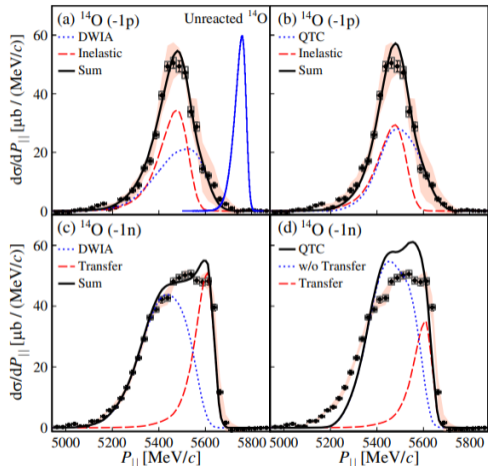
(c)(d)

(deeply bound) 1n removal:

low-momentum tail and

high-momentum sharp edge.

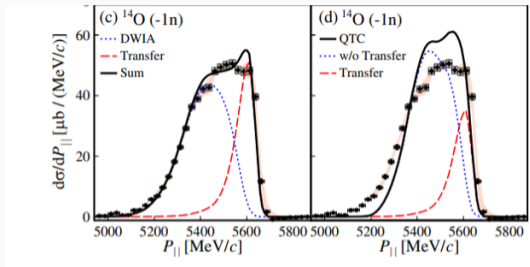
# Parallel momentum distributions of $^{13}\text{N}$ and $^{13}\text{O}$



(a)(b) 1p removal:

- Considered the  $(p, p')$  inelastic excitation of  $^{14}\text{O}$  to its low-lying excited states, emit one proton to get  $^{13}\text{N}$ .
- Large contribution of inelastic scattering: 51% with DWIA, 43% with QTC.
- If ignore inelastic scattering:  $R_s$  is around unity, equivalent to eikonal model.
- Use multiparticle-multipole configurations to describe low-lying excited states.
- Beyond the  $(p, pN)$  and the eikonal models, which assume the projectile is a single-particle state plus an inert core.

# Parallel momentum distributions of $^{13}\text{N}$ and $^{13}\text{O}$



(c)(d)  $1n$  removal:

- Perform QTC with outgoing channel coupled only to deuteron ground state: equivalent to DWBA.
- QTC  $\sigma_{sp}$  without the  $(p, d)$  transfer is still larger than the DWIA result.

Symmetrical properties:

- Low-momentum tail is caused by the attractive potential between the outgoing nucleons and  $^{13}\text{O}$ .
- Due to the two-body kinematics of the transfer reaction, transfer reaction creates a sharp high-momentum edge, which is inaccessible to knockout.
- QTC reproduces better the sharp high-momentum side, since it treats  $(p, d)$  transfer consistently with  $(p, pn)$ .

# $R_s$ as a function of $\Delta S$

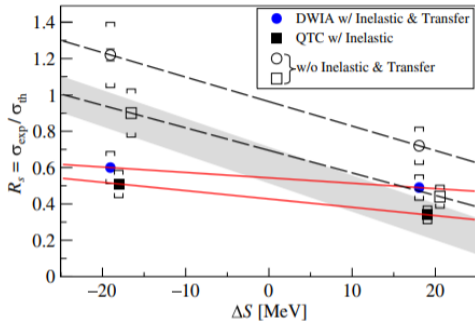


FIG. 3.  $R_s$  as a function of  $\Delta S$  from the present work (blue dots and black squares) compared to the trend extracted from Be or C induced nucleon-removal cross sections analyzed with the eikonal model [19–21] (gray shaded region). The square brackets indicate the total systematic uncertainties. Red solid and black dashed lines are shown to guide the eyes.

- Eikonal model: gray shaded area. Slope is  $-1.6 \times 10^{-2} \text{ MeV}^{-1}$  for light-ion induced nucleon removal.
- Analyses of low-energy one-nucleon transfer and high energy quasifree scattering data: slope is  $(10^{-3} - 10^{-5}) \text{ MeV}^{-1}$
- Present work: DWIA and QTC with inelastic and transfer:  $R_s$  have a weak  $\Delta S$  dependence; the slope is  $-3.0(5)(5) \times 10^{-3} \text{ MeV}^{-1}$  and  $-4.6(4)(7) \times 10^{-3} \text{ MeV}^{-1}$  respectively.
- Neglect inelastic and transfer: slopes are 3–5 times larger.